Rend. Sem. Mat. Univ. Politec. Torino
Vol. 69, 1 (2011), 21 – 35

N. Akroune

ON THE DYNAMICS OF A PERTURBED HOLOMORPHIC DYNAMICAL SYSTEM

Abstract. The purpose of this work is to study the dynamics of a discrete bidimensional dynamical system which depends on a real parameter. This system is obtained by a perturbation of a holomorphic polynomial whose Julia set is well known. The attractors of the initial system, as well as their attractive basins, are determined. Different types of bifurcations are identified.

1. Introduction

The holomorphic dynamical systems generated by rational functions have been intensively studied ever since the pioneering works of G. Julia [9] and P. Fatou [7].

In another context, the discrete bidimensional dynamical systems are modelled by noninvertible (piecewise continuous, continuous or differentiable) maps T. Such a map T is defined by

$$\begin{array}{rccl} T: & \mathbb{R}^2 \supseteq S & \longrightarrow & S \\ & (x,y) & \rightsquigarrow & (f_1(x,y),\, f_2(x,y)). \end{array}$$

The dynamical system $(S,\mathbb{N},T)$ is holomorphic if T is differentiable and if its two components $(f_i,\ i=1,2)$ satisfy the *Cauchy–Riemann* conditions.

In the light of recent developments of the theory (see [13, 1, 10, 8, 3, 11]), we present a study on the dynamics of a system generated by a map T that depends continuously on a real parameter. The choice of T is motivated by the fact that when the parameter is equal to zero, the map T can be viewed as an holomorphic one. In addition to a comparison with the last system, the dynamics, stability and attractors of the initial one will be presented for some range of the parameter. We will show that the attractors of this system are of different types (fixed points, periodic points, closed invariant curves, chaotic attractors). Local and global bifurcations are encountered when varying the parameter.

The plan is as follows. In Section 2, we present the two-dimensional recurrence T and its particularities. Section 3 is devoted to the determination of the critical curve of the present case. In Section 4, we calculate the fixed and periodic points depending on the parameter of the system. When this parameter is modified in the range of interest, we treat successively the appearance/disappearance of closed invariant curves and cycles (Section 5) and the birth of a chaotic attractor (Section 6), with presentation of the associated figures. The last section contains a conclusion and a proposed generalization of this study.

2. The model

The bidimensional transformation considered in this work is :

$$\begin{array}{rccl} T_{a,b,\alpha}\colon & \mathbb{R}^2 & \longrightarrow & \mathbb{R}^2 \\ & (x,y) & \rightsquigarrow & (x^2-y^2+a+\alpha y,\ 2xy+b+\alpha x) \end{array} \tag{1}$$

with $(a,b)\in\mathbb{R}^2$ and $\alpha\in\mathbb{R}^*$. In the sequel, we shall sometimes write either T in place of $T_{a,b,\alpha}$ as the dependence of T on the parameters a,b,α is understood.

The expression of T can evidently be written in the more explicit form

$$T\begin{pmatrix} x \\ y \end{pmatrix} = \begin{pmatrix} x^2-y^2+a \\ 2xy+b \end{pmatrix} + \alpha \begin{pmatrix} y \\ x \end{pmatrix},$$

so if $\alpha = 0$, we can simply write

$$T_{a,b,0}(x,y) = T_c(z = x+iy) = z^2 + c,$$

with $c = a+ib \in \mathbb{C}$. In other words, the initial dynamical system (1) becomes a holomorphic one; the properties of this particular case (fixed and periodic points, Julia set, etc.) are explained in detail in the literature (see for instance [5, 4, 6]).

If $\alpha \neq 0$, the transformation T can also be written $T_{c,\alpha}(z) = z^2 + c + i\alpha\bar{z}$, i.e. T is now a nonholomorphic map. Interesting studies on a special form of these types of systems have been proposed by K. Uchimura [18, 17, 16].

3. The critical curve of a noninvertible map

3.1. Some considerations on the degree of a mapping

In this subsection, we will consider only proper smooth maps $f : \mathbb{R}^n \longrightarrow \mathbb{R}^n$. (In this setting, "proper" means $\|f(x)\| \to \infty$ when $\|x\| \to \infty$.) A *regular* point of a differentiable map f is a point at which the Jacobian determinant $J_f(x) \neq 0$. The set R_f of all regular points of f is open. Its complement is the set C_f of *critical points* of the map f. A *regular value of an* f-map is a point of the range whose pre-images consist of regular points, otherwise the point is a *critical value*. Since the set of critical points is closed and since proper maps send closed sets into closed sets, it follows that the set of critical values $LC = f(C_f)$ is closed and hence, the set of regular values of a proper differentiable map is open. Moreover it is dense by Sard's theorem.

Given a proper differentiable map $f : \mathbb{R}^n \longrightarrow \mathbb{R}^n$, the *mapping degree* (also called *Brouwer degree*) of f is the integer

$$\deg(f) = \sum_{x\in f^{-1}(y)} \operatorname{sgn}(J_f(x))$$

where y is any regular value of f. This number is independent of the choice of the regular value y. (Further details can be found in [12].)

Let us define the *multiplicity* $m(f) \in \mathbb{N} \cup \{\infty\}$ by

$$m(f) = \sup\{\text{cardinality}(f^{-1}(y)) : y \in \mathbb{R}^n\}.$$

If $n = 2$ and f is holomorphic then $\deg(f) = m(f)$, since $\text{sgn}(J_f(x))$ equals 1 everywhere. However, for the map $g(x,y) = (x^2, y)$ we have $\deg(g) = 0$ but $m(g) = 2$.

For holomorphic maps, the locus $LC = f(C_f)$ coincides with the set of points which have at least two merging predecessors (e.g. $u(z) = z^3$). However one cannot say this of the map $h(x,y) = (x^3, y)$, which is a homeomorphism.

3.2. On the critical curve of a two-dimensional noninvertible map

The existence of the critical curve (abbreviated *LC* for "**L**igne **C**ritique" in French) is one of the distinguishing features of any noninvertible two-dimensional map G (not just the map T given by (1)). It was introduced by C. Mira in 1964 (see [13] and references therein). The phase space can be divided into open regions $(Z_k)_{k\in\mathbb{N}}$ in which points have k rank-one preimages under the map G, and these regions are separated by LC. The latter curve plays a fundamental role in determining the properties and the global bifurcations of basins [10, 8]. When the map G is continuously differentiable, we have $LC = G(LC_{-1})$ where LC_{-1} is identical to the set C_G above, and the maximum value of the integer k is given by the multiplicity $m(G)$.

3.3. The critical curve of our model

In the present case, the transformation T of (1) is differentiable, so LC is the image of the locus LC_{-1} of points where the determinant of the Jacobian matrix of T vanishes. At a point (x,y), this matrix takes the form

$$J(x,y;\alpha) = \begin{pmatrix} 2x & \alpha - 2y \\ \alpha + 2y & 2x \end{pmatrix}, \tag{2}$$

and LC_{-1} is the curve whose points (x,y) verify $\det(J(x,y;\alpha)) = 0$. Such points satisfy the equation

$$4(x^2 + y^2) - \alpha^2 = 0.$$

Therefore

$$LC_{-1} = \left\{ (x,y) \in \mathbb{R}^2 : x^2 + y^2 = \left(\frac{\alpha}{2}\right)^2 \right\}$$

is the circle centered at $(0,0)$ with radius $\alpha/2$, and the critical curve can be parametrized as follows:

$$LC = T_{a,b,\alpha}(LC_{-1}) = \{(u(t), v(t)),\ t \in [0,\ 2\pi]\},$$

with

$$\begin{cases} u(t) = \dfrac{\alpha^2}{4}\cos 2t + \dfrac{\alpha^2}{2}\sin t + a \\ v(t) = \dfrac{\alpha^2}{4}\sin 2t + \dfrac{\alpha^2}{2}\cos t + b. \end{cases}$$

As Y varies in $\mathbb{R}^2\backslash LC$, we can show that the equation $T(X) = Y$ admits only two or four solutions (i.e. $m(T) = 4$); the map T is of the type $(Z_2 - Z_4)$ according to the nomenclature established by Mira [13]. The phase space can be separated in two distinct connected (or multiply-connected) zones (Z_2 and Z_4) in which each point has two or four preimages under T, that is $(\mathbb{R}^2 = \overline{Z_2} \cup \overline{Z_4})$. Note that the curve has three cusp points whose coordinates are $(-\frac{3}{4}\alpha^2, 0)$ and $(\frac{3}{8}\alpha^2, \pm\frac{3\sqrt{3}}{8}\alpha^2)$; at these points, T has three coincident preimages. An example of such curve is shown in Figure 1; it is formed by the points which have at least two coincident preimages and is similar to Steiner's hypocycloid [18].

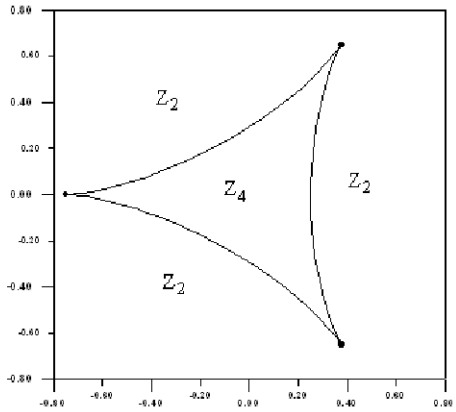

Figure 1: The critical curve LC for $a = b = 0$ and $\alpha = 1$. The three cusp points are plotted with big dots; each point in Z_4 admits four distinct preimages under the map T

4. Fixed points and periodic points

When $(a,b) \in \mathbb{R}^2$ and $\alpha \in \mathbb{R}^*$, the fixed points $X^* = (x^*, y^*)$ of the system are given by

$$y^* = \frac{\alpha x^* + b}{1 - 2x^*}, \tag{3}$$

where x^* verifies the polynomial equation

$$4x^4 - 8x^3 + (5 + 4a - 3\alpha^2)x^2 + (\alpha^2 - 4\alpha b - 4a - 1)x + (a + \alpha b - b^2) = 0 \tag{4}$$

of degree 4 (4 being the degree of the map T).

To study their stability, we must consider the modulus of the eigenvalues of the Jacobian matrix (see (2)). Its characteristic polynomial is

$$U_\lambda(x,y) = \lambda^2 - 4x\lambda + [4(x^2 + y^2) - \alpha^2]. \tag{5}$$

We remark that $U_\lambda(x,y) = U_\lambda(x,-y)$; let us note that this property will be used in the next subsection.

4.1. The particular case $a = b = 0$

In this study, we restrict investigation to the particular case $a = b = 0$. Indeed:

i) The Jacobian matrix (2), and consequently the characteristic polynomial (5), does not depend *explicitly* on a or b.

ii) The determination of the fixed points of T is less difficult (see (3) and (4)).

iii) The trivial case $(a = b = \alpha = 0)$ transforms the map T into the quadratic complex polynomial $T(z = x + iy) = H(z) = z^2$.

We recall that the *Julia set* (see [9, 6]) of H is simply the unit circle: this invariant set separates the immediate attracting basins of the origin and the point at infinity. In the next subsection, we shall see the form of the first basin when α is close to *zero*.

With these changes (i.e. $a = b = 0$ and $\alpha \neq 0$), the expression of T becomes

$$T_\alpha(x,y) = \Big(f_\alpha(x,y) = x^2 - y^2 + \alpha y,\ \ g_\alpha(x,y) = 2xy + \alpha x \Big).$$

It is easy to see that for all $(x,y) \in \mathbb{R}^2$ and for all $\alpha \in \mathbb{R}^*$, we have

$$f_\alpha(x,y) = f_{-\alpha}(x,-y) \tag{6}$$

$$g_\alpha(x,y) = -g_{-\alpha}(x,-y). \tag{7}$$

In complex notation, these two equalities give us the important property

$$T_\alpha(z) = \overline{T_{-\alpha}(\overline{z})} \tag{8}$$

where $z = x + iy$.

PROPOSITION 1. *If (v,w) is a fixed point of T_α then $(v,-w)$ is a fixed point of $T_{-\alpha}$ and these both points have the same multipliers.*

Proof. The first statement comes directly from (6)–(8), and the remark which follows (5) proves the second part. □

This last proposition can be generalized as follows:

PROPOSITION 2. *If (v,w) is a k-periodic point of T_α (with $k \geq 2$) then $(v,-w)$ is also a k-periodic point of $T_{-\alpha}$ and both points have the same multipliers.*

Proof. For example, with $k = 2$, we obtain the following equalities

$$\begin{aligned}
T^2_{-\alpha}(v,-w) &= T_{-\alpha}(T_{-\alpha}(v,-w)) \\
&= T_{-\alpha}(f_{-\alpha}(v,-w),\ g_{-\alpha}(v,-w)) \\
&\overset{(6)-(7)}{=} T_{-\alpha}(f_\alpha(v,w),\ -g_\alpha(v,w)) \\
&\overset{(8)}{=} T_\alpha(f_\alpha(v,w),\ g_\alpha(v,w)) \\
&= T^2_\alpha(v,w).
\end{aligned}$$

The last part of the assertion follows from (5) and the chain rule of differentials. □

From these two propositions, it follows

COROLLARY 1. *In terms of the real parameter* α*, the study of the behavior of the dynamical system* $(\mathbb{R}^2, \mathbb{N}, T_\alpha)$ *can be reduced to the interval* $]0, +\infty[$*. In other words, the dynamics of the maps* T_α *and* $T_{-\alpha}$ *are essentially the same (see* (8)*).*

4.2. The fixed points of T_α with $\alpha > 0$

The origin $O = (0, 0)$ is obviously a fixed point of T_α, and its multipliers (see *eq*. 5) are deduced from the expression of $U_\lambda(0, 0) = \lambda^2 - \alpha^2$. Therefore, if $\alpha < 1$ the origin is an attractive node, and is, in particular, a hyperbolic fixed point.

As regards other fixed points (x^*, y^*): (3) and (4) become respectively

$$y^* = \frac{\alpha x^*}{1-2x^*},$$
$$4x^3 - 8x^2 + (5-3\alpha^2)x + (\alpha^2 - 1) = 0,$$

so that x^* now verifies a polynomial equation $L(x) = 0$ of degree 3. We stress here that $x = 1/2$ cannot be a root of L, otherwise the parameter α would equal 0.

This cubic equation admits at least one real root $\widehat{x}$, its expression is given by

$$\widehat{x} = \widehat{x}(\alpha) = \frac{2}{3} + \frac{K}{6} + \frac{1/6 + 3\alpha^2/2}{K},$$

where

$$K = K(\alpha) = \left(1 + 27\alpha^2 + 3\alpha\sqrt{3 + 54\alpha^2 - 81\alpha^4}\right)^{\frac{1}{3}}.$$

REMARK 1. If $\alpha \to 0$ then $K(\alpha) \to 1$ and this leads to $(\widehat{x}(\alpha), \widehat{y}(\alpha)) \longrightarrow (1, 0)$ which is the repulsive fixed point of $H(z) = z^2$.

Let $\widehat{\alpha}$ be the unique positive root of the argument inside $\sqrt{3 + 54\alpha^2 - 81\alpha^4}$, the square root that appears in the above expression of K, that is

$$\widehat{\alpha} = \frac{1}{3}\sqrt{3 + 2\sqrt{3}} \approx 0.84748\ldots$$

Numerical calculations allow us to establish that the map T possesses, in addition to the origin O, one (resp. two, resp. three) real fixed point(s) when $\alpha < \widehat{\alpha}$ (resp. $\alpha = \widehat{\alpha}$, resp. $\alpha > \widehat{\alpha}$). When α crosses the value $\widehat{\alpha}$, one of the both fixed points admits $\lambda = 1$ as a multiplier: this indicates a fold-bifurcation.

Figure 2(a) shows the attractive basin of the origin for $(\alpha = 0.1)$, the point

$$\left(\widehat{x},\, \widehat{y} = \frac{\alpha\widehat{x}}{1-2\widehat{x}}\right) = (1.0190\ldots,\, -0.0981\ldots)$$

belongs to the basin boundary. In the following paragraph, we discuss the properties of the maps T_α and H near to the origin.

On the existence of a local topological conjugacy between T_α and H. Consider the map T_α as a 2-dimensional real map, we denote by $\mathscr{L}(T_\alpha)(x,y) = (\alpha y,\ \alpha x)$ the linear part of T_α.

For $\alpha > 0$ small, the mapping $\mathscr{L}(T_\alpha)$ is clearly invertible and attracting in the neighborhood of the origin, so one can apply the Grobman–Hartman theorem (for maps, see [15]) to infer that the map T_α is locally topologically conjugated to its linear part, not to its quadratic part. Furthermore, being locally invertible because the linear part is, the map T_α cannot be topologically conjugated to the quadratic map $H(z) = z^2$ (also viewed as a 2-dimensional real map), which is not locally invertible near the origin $(\det(J_H(0,0)) = 0)$.

Although the two systems are not locally topologically conjugated, the basin of attraction of the hyperbolic fixed point O is quite similar to the unit disk (the Julia set of H), this fact is illustrated in Figure 2 for different parameter values.

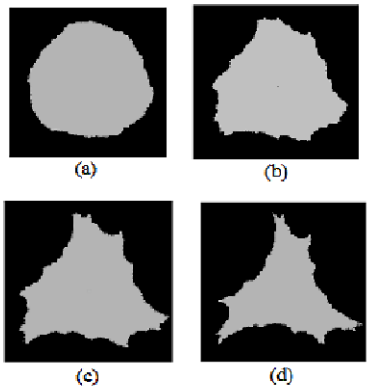

Figure 2: Phase portraits of T_α for (a) $\alpha = 0.1$, (b) $\alpha = 0.3$, (c) $\alpha = 0.5$, (d) $\alpha = 0.8$. In each case, the grey region represents the attractive basin of O (located at the center of the square), and all the iterates (in the black area) go to the point at infinity

4.3. Saddle and cycle of order 2

Beyond the value $\widehat{\alpha}$, all the stationary points of T are real. Analyzing their stability, we observe that, for $\widehat{\alpha} < \alpha < \beta = 0.95280\ldots$, the dynamical system has, in addition to the origin, a stable focus and two other repelling fixed points (a saddle and an instable focus). In parallel to these four fixed points, we remark, by solving the equation $T_\alpha^2(x,y) = (x,y)$ when $\alpha \in]\widehat{\alpha}, \beta[$, the appearance of an attracting cycle of order 2. An example of this behavior is depicted in Figure 3 for $\alpha = 0.9$, the related numerical values (of the fixed and periodic points) are summarized in the table below :

Point	Type	Stability
$O = (0, 0)$	Fixed point	Attracting node
$(1.6219\ldots, -0.6505)$	Fixed point	Instable focus
$(0.1087\ldots, 0.1250\ldots)$	Fixed point	Saddle
$(0.2693\ldots, 0.5254\ldots)$	Fixed point	Stable focus
$(0.3204\ldots, -0.4960\ldots)$	2-periodic	Attracting cycle
$(-0.5897\ldots, -0.0294\ldots)$	2-periodic	Attracting cycle

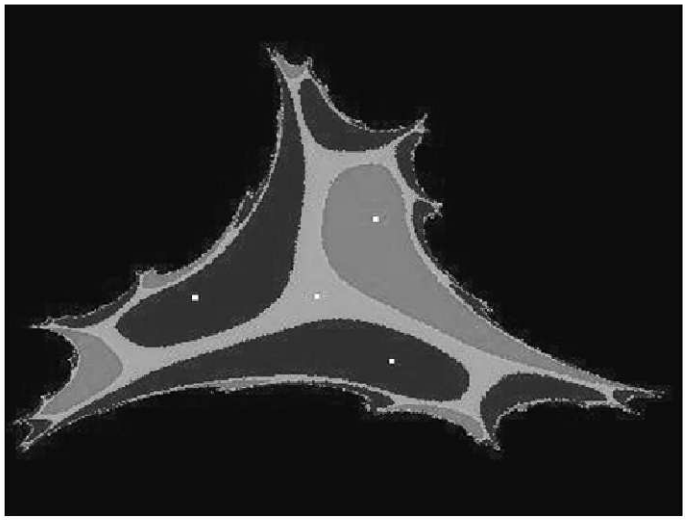

Figure 3: For $\alpha = 0.9$, the map T admits three stable sets at finite distance: the origin, a focus and a 2-attracting cycle. Their respective basins are represented by distinct shading: light grey, grey and dark grey

REMARK 2. Note that Figures 2–6 and Figure 9 are included in the square $[-2.5, 2.5] \times [-2.5, 2.5]$.

5. Closed invariant curves and cycles

5.1. Closed invariant curves

The previous attracting 2-cycle loses its stability at a bifurcation value ($\beta = 0.95280\ldots$), and then the system generates three smooth (i.e. with no self-intersections points) C.I.C. (Closed Invariant Curves, see [1]): the system undergoes the so-called Neimark–Sacker bifurcation. This new behavior is observed in the interval $]\beta, \gamma = 1.0153\ldots[$. Two of these curves have the same attracting basin, while the third has its own one.

However, we recall that the origin is stable (resp. unstable) when $\alpha < 1$ (resp. $\alpha > 1$), and therefore the system possesses three (resp. two) stable sets at finite distance.

As an illustration for the (critical) value $\alpha = 1$, the precedent stable focus (see the above table) becomes instable and is surrounded by a stable curve. The other curves form an attracting set and the system evolves alternately on them (see Figure 4).

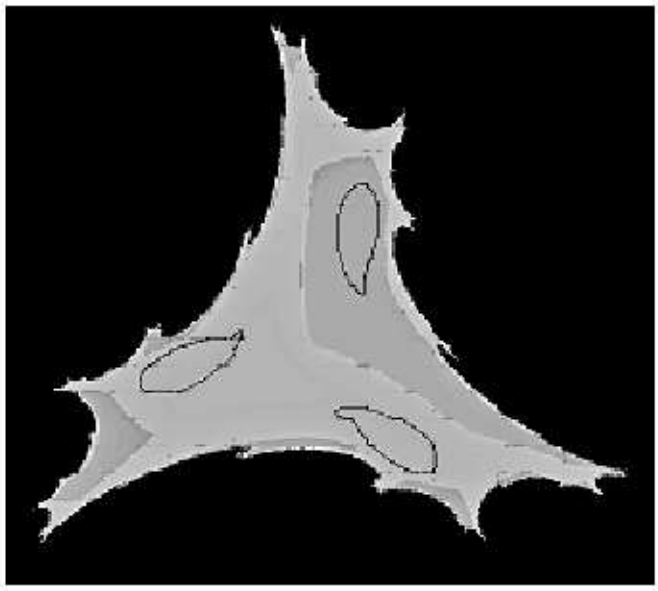

Figure 4: The dynamics of T for $\alpha = 1$: three smooth C.I.C.'s and their two respective attracting basins (in light and dark grey). The basin of infinity is in black. Note that the origin is unstable and belongs to the basin boundary of the top curve

5.2. Other periodic points

Another bifurcation occurs when the parameter α is increased very slightly, starting from γ. The previous set of three curves disappears completely and is replaced by periodic points of high order l $(l \geq 9)$. In fact, two distinct stable cycles of different order coexist and divide the phase portrait into two attracting basins (see Figure 5); this situation is observed in the interval $]\gamma,\ \mu = 1.02673\ldots[$. It should be noted that the bifurcations values (β, γ and μ) are close to each other.

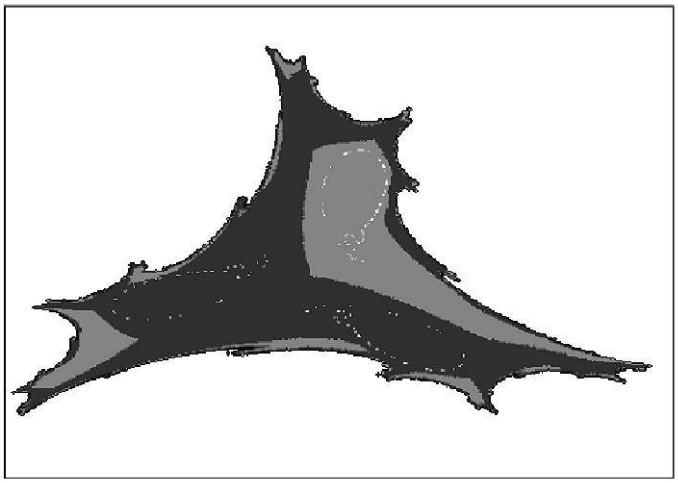

Figure 5: For $\alpha = 1.02$, the map T admits two stable cycles of order 19 and 38

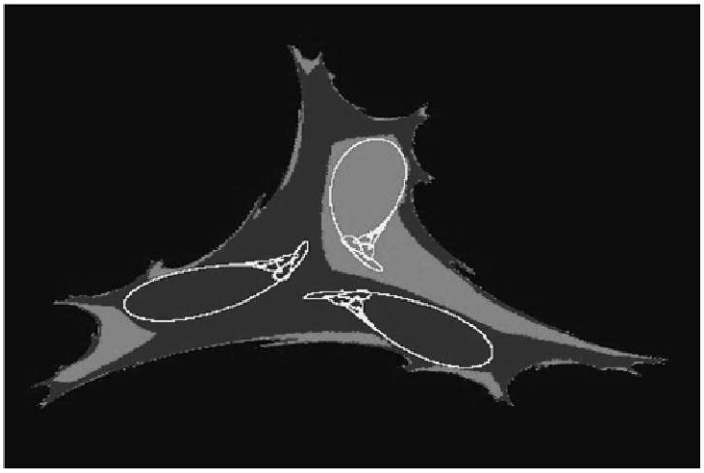

Figure 6: Loss of smoothness of each C.I.C.; the system presents a chaotic behavior on them. Two curves have the same basin (in dark grey). As in Figure 5, the black region is the basin of infinity. The parameter value is set to $\alpha = 1.031$

6. Transition to chaos

There exist many ways in which a dynamical system can present a chaotic behavior. Among them, the period-doubling route to chaos is the well-known. Another scenario, encountered in our study, is the progressive destruction of a closed invariant curve and its transformation into a chaotic attractor [1].

As the parameter α is varied in the interval $]\mu = 1.02673\ldots,\ \omega = 1.03777\ldots[$, the three C.I.C. (identified in the present model, see the previous section) reappear once again, but with the loss of their smoothness. By a mechanism explained in detail in [3, 11], one sees progressively the appearance of cusp points on each curve, followed by the generation of loops (or self-intersections) (see Figure 6). The critical curves (LC) (see Section 3), play an important role in these transformations (see [1, 11]).

It is worth noting that, as reported in the end of the above section, all these changes take place for very small parameter ranges.

Beyond the value $\omega = 1.03777\ldots$, we note the birth of a chaotic attractor (see Figure 7). This invariant set is formed by the connection of the previous nonsmooth C.I.C. It presents clearly a fractal structure (see Figure 8). Besides, its capacity (resp. information) dimension, which is estimated for $\alpha = 1.04$ by a variant of the box-counting algorithm (proposed in [2]), has the value $D_{Cap} \approx 1.46$ (resp. $D_{Inf} \approx 1.40$).

The previous chaotic attractor subsists in the interval $]\omega,\ \delta = 1.066\ldots[$, and then a contact bifurcation occurs (see [1]). This bifurcation takes place in the contact between the chaotic set and its basin boundary (see Figure 9). Beyond the value δ, the chaotic attractor is destroyed and all the trajectories diverge for almost any initial condition $(x_0, y_0) \in \mathbb{R}^2$.

REMARK 3. The detection of each of the values $(\beta, \gamma, \mu, \omega, \delta)$ of the parameter α, on which particular types of phase portraits arise, was done using a *Fortran 90* program. By scanning the interval $\alpha > 0$, several (numerical and graphical) experiments were performed. In addition, the software *Dynamics–Smalldyn* [14] was very helpful in the development of the graphical representations.

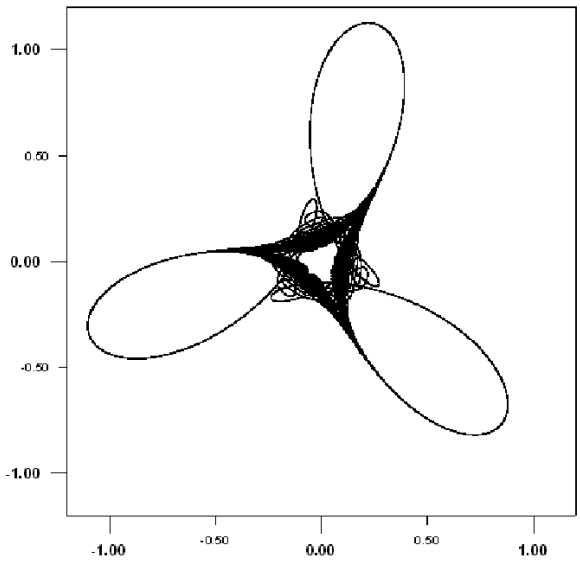

Figure 7: $\alpha = 1.04$. A typical chaotic attractor of T (80,000 points are plotted)

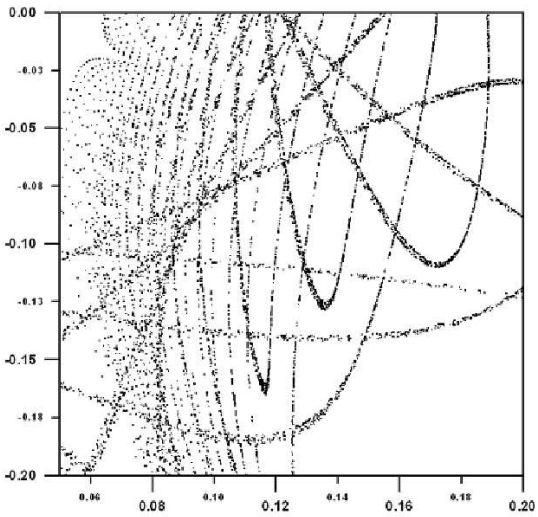

Figure 8: A magnification of a part of the chaotic set (Figure 7), corresponding to the rectangle $[0.05, 0.20] \times [-0.20, 0.00]$

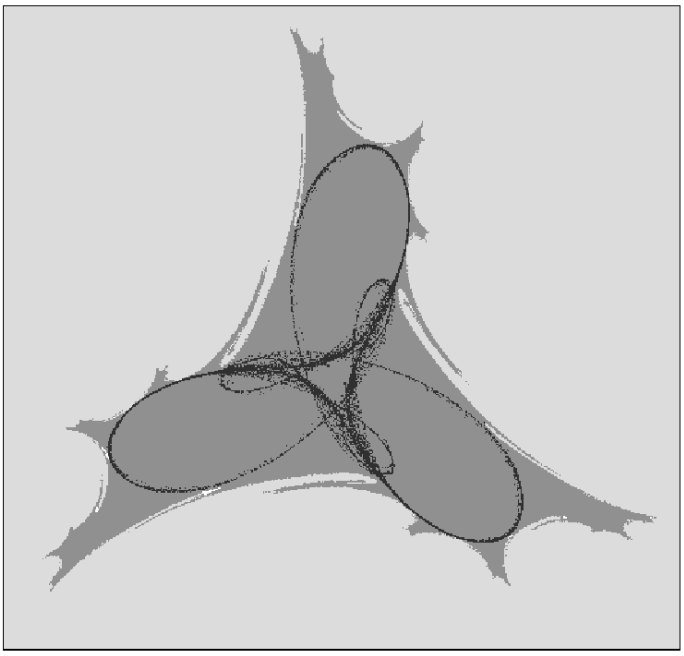

Figure 9: $\alpha \approx 1.0655$: just before the contact bifurcation of the chaotic attractor with its basin boundary

Conclusion

Our aim was to study the dynamics of a perturbed holomorphic map which depends continuously on a real parameter. In this context, we focused on the attractive basins and their boundaries. When the parameter is close to zero, the map T has some properties similar to those of the associated holomorphic dynamical system, even if these two systems are not topologically conjugate.

Although the initial system has only one parameter, we noticed that it presents a great complexity in its behavior: the attractors are regular (equilibria, stable cycles, closed invariant curves) or chaotic. In particular, the process of the appearance or disappearance of the closed invariant curves is clarified by graphical representations.

We can consider another form of (1), that is:

$$T_{a,b;\alpha,\beta}(x,y) = (x^2 - y^2 + a + \alpha y,\ \ 2xy + b + \beta x),$$

with $(a,b) \in \mathbb{R}^2$ and $(\alpha,\beta) \in (\mathbb{R}^*)^2$. If $\alpha = \beta = 0$, one also find the well studied quadratic map $T_{a,b;0,0}(x,y) = T(z) = z^2 + c$ (with $z = x + iy$ and $c = a + ib \in \mathbb{C}$). For a fixed pair (a,b), it may be possible to build the bifurcation diagram in the parameter (α,β)-plane, in parallel with the representative phase portraits.

Acknowledgments. The author would like to thank the referee for his careful reading of the work and his pertinent remarks.

References

[1] AGLIARI A., BISCHI G. I. AND GARDINI L. Chapter 1. Some methods for the global analysis of closed invariant curves in two-dimensional maps. In *Business Cycle Dynamics – Models and Tools*, T. Puu and I. Sushko, Eds. Springer-Verlag, Berlin, 2006.

[2] AKROUNE N. Sur une variante de la méthode des boîtes pour la détermination numérique de la dimension fractale d'un sous-ensemble du plan. *C. R. Math. Acad. Sci. Paris 338*, 11 (2004), 899–904.

[3] BISCHI G. I. AND VALORI V. Nonlinear effects in a discrete-time dynamic model of a stock market. *Chaos Solitons Fractals 11*, 13 (2000), 2103–2121.

[4] BLANCHARD P. Complex analytic dynamics on the Riemann sphere. *Bull. Amer. Math. Soc. 11*, 1 (1984), 85–141.

[5] BROLIN H. Invariant sets under iteration of rational functions. *Ark. Mat. 6* (1965), 103–144.

[6] DEVANEY R. L. *An Introduction to Chaotic Dynamical Systems*. Addison-Wesley, Redwood City, CA, 1989. 2nd edition.

[7] FATOU P. Sur les équations fonctionnelles. *Bull. Soc. Math. France 47; 48* (1919; 1920), 161–271; 33–94, 208–314.

[8] GARDINI L., ABRAHAM R., RECORD R. AND FOURNIER-PRUNARET D. A double logistic map. *Internat. J. Bifur. Chaos Appl. Sci. Engrg. 4*, 1 (1994), 145–176.

[9] JULIA G. Mémoire sur l'itération des fractions rationnelles. *J. Math. Pures Appl. 8* (1918), 47–245.

[10] LOPEZ-RUIZ R. AND FOURNIER-PRUNARET D. Complex pattern on the plane: different types of basin fractalization in a two-dimensional mapping. *Internat. J. Bifur. Chaos Appl. Sci. Engrg. 13*, 2 (2003), 287–310.

[11] MAISTRENKO V., MAISTRENKO Y. AND MOSEKILDE E. Torus breakdown in noninvertible maps. *Phys. Rev. E (3) 67*, 4 (2003), 046215.

[12] MILNOR J. W. *Topology from the Differentiable Viewpoint*. Princeton Landmarks in Mathematics. Princeton University Press, Princeton, 1997. Revised reprint of the 1965 original.

[13] MIRA C., GARDINI L., BARUGOLA A. AND CATHALA J. C. *Chaotic dynamics in two-dimensional noninvertible maps*, vol. 20 of *World Scientific Series on Nonlinear Sciences, Series A*. World Scientific, River Edge, NJ, 1996.

[14] NUSSE H. E. AND YORKE J. A. *Dynamics: Numerical Explorations*. Applied Mathematical Sciences 101. Springer-Verlag, New York, 1997. 2nd edition.

[15] TESCHL G. *Ordinary Differential Equations and Dynamical Systems*. Graduate Studies in Mathematics. Amer. Math. Soc., Providence RI, 2011 to appear.

[16] UCHIMURA K. The dynamical systems associated with Chebyshev polynomials in two variables. *Internat. J. Bifur. Chaos Appl. Sci. Engrg. 6*, 12B (1996), 2611–2618.

[17] UCHIMURA K. Attracting basins of certain nonholomorphic maps. *Internat. J. Bifur. Chaos Appl. Sci. Engrg. 8*, 7 (1998), 1517–1526.

[18] UCHIMURA K. Filled Julia sets of certain nonholomorphic maps. Preprint 015, Report, Math. Tokai Univ., 1999.

AMS Subject Classification: 37Exx, 37F45, 37G35

Nourredine AKROUNE
Department of Mathematics, Laboratory of Applied Mathematics
University of Bejaia, 06000 ALGERIA
e-mail: akroune_n@yahoo.fr

Lavoro pervenuto in redazione il 03.01.2011 e, in forma definitiva, il 13.06.2011